Geobiology (2004), **2**, 163–177

Linking geochemical processes with microbial community analysis: successional dynamics in an arsenic-rich, acid-sulphate-chloride geothermal spring

R. E. MACUR, H. W. LANGNER, B. D. KOCAR AND W. P. INSKEEP

Thermal Biology Institute and Department of Land Resources and Environmental Sciences, Montana State University – Bozeman, Bozeman, Montana 59717, USA

ABSTRACT

The source waters of acid-sulphate-chloride (ASC) geothermal springs located in Norris Geyser Basin, Yellowstone National Park contain several reduced chemical species, including H_2, H_2S, As(III), and Fe(II), which may serve as electron donors driving chemolithotrophic metabolism. Microorganisms thriving in these environments must also cope with high temperatures, low pH (~3), and high concentrations of sulphide, As(III), and boron. The goal of the current study was to correlate the temporal and spatial distribution of bacterial and archaeal populations with changes in temperature and geochemical energy gradients occurring throughout a newly formed (redirected) outflow channel of an ASC spring. A suite of complimentary analyses including aqueous geochemistry, microscopy, solid phase identification, and 16S rDNA sequence distribution were used to correlate the appearance of specific microbial populations with biogeochemical processes mediating S, Fe, and As cycling and subsequent biomineralization of As(V)-rich hydrous ferric oxide (HFO) mats. Rapid As(III) oxidation (maximum first order rate constants ranged from 4 to 5 min^{-1}, $t_{1/2}$ = 0.17 – 0.14 min) was correlated with the appearance of *Hydrogenobaculum* and *Thiomonas*–like populations, whereas the biogenesis of As(V)-rich HFO microbial mats (mole ratios of As:Fe ~0.7) was correlated with the appearance of *Metallosphaera*, *Acidimicrobium*, and *Thiomonas*–like populations. Several 16S sequences detected near the source were closely related to sequences of chemolithotrophic hyperthermophilic populations including *Stygiolobus* and *Hydrogenobaculum* organisms that are known H_2 oxidizers. The use of H_2, reduced S(–II,0), Fe(II) and perhaps As(III) by different organisms represented throughout the outflow channel was supported by thermodynamic calculations, confirming highly exergonic redox couples with these electron donors. Results from this work demonstrated that chemical energy gradients play an important role in establishing distinct community structure as a function of distance from geothermal spring discharge.

Received 27 April 2004; accepted 12 August 2004

Corresponding author: W. P. Inskeep, tel.: 406-994-5077; fax: 406-994-3933; e-mail: binskeep@montana.edu

INTRODUCTION

Source waters of geothermal springs are generally far from thermodynamic equilibrium with respect to earth-surface conditions, resulting in thermal and chemical energy gradients that drive a variety of abiotic and microbially mediated reactions. Many chemical constituents present in geothermal waters undergo abiotic reactions including oxidation with O_2, and release of oversaturated constituents via degassing or precipitation. However, numerous oxidation-reduction processes important in geochemical cycling are also catalysed by microorganisms, where reduced species such as H_2, H_2S, S°, Fe(II), and As(III) may serve as electron donors for energy conservation, and oxidized species such as O_2, NO_3^-, SO_4^{2-}, and As(V) may be reduced during respiration (Amend & Shock, 2001). In addition, potentially toxic elements such as As may be transformed by microbial processes associated with detoxification rather than energy conservation (Silver, 1996; Mukhopadhyay *et al.*, 2002; Rosen, 2002). In many cases, the relative importance of abiotic and biotic processes varies for specific constituents as a function of temperature and distance down gradient from spring discharge, creating numerous unique thermal and geochemical environments that serve as niches for possible microbial specialization.

The source waters of acid-sulphate-chloride (ASC) geothermal springs located in the Norris Geyser Basin of Yellowstone

National Park (YNP) contain variable concentrations of reduced chemical species including H_2, H_2S, As(III) and Fe(II) in a background solution containing millimolar levels of Na^+, SO_4^{2-} and Cl^- (Ball *et al.*, 2002; Stauffer *et al.*, 1980; Langner *et al.*, 2001). The combination of high temperature, low pH (~3), high sulphide, high As(III), and elevated levels of other trace elements such as B create an extreme environment where chemolithoautotrophs dependent on inorganic constituents for energy generation and CO_2 as a C source are likely the dominant primary producers (Langner *et al.*, 2001; Amend & Shock, 2001). Microorganisms adapted to these unique and extreme geothermal environments may exhibit metabolic strategies that are quite different than those used by many of the microorganisms in culture (e.g. Horikoshi & Grant, 1998; Huber *et al.*, 2000; Amend & Shock, 2001). Consequently, considerable effort has recently focused on describing novel 16S rDNA sequences and or isolates from extreme environments, as well as the ecology and geochemistry of these unusual habitats (e.g. Reysenbach & Shock, 2002; Horikoshi & Grant, 1998; Huber *et al.*, 2000; Jackson *et al.*, 2001; Langner *et al.*, 2001).

Recent molecular and geochemical characterization of a representative ASC thermal spring (*Dragon Spring*) in Norris Basin showed that microbial mat communities changed dramatically with distance down the outflow channel correlating with major changes in aqueous and solid phase geochemistry (Jackson *et al.*, 2001; Langner *et al.*, 2001). While no As(III) oxidation was observed within the S° depositional zone (0–3 m), *in situ* microbial oxidation of As(III) to As(V) occurred at rates faster than ever reported for natural waters immediately down gradient at 4–5 m ($t_{1/2}$ ~0.6 min; Langner *et al.*, 2001). Results from electron microscopy (SEM/EDAX), X-ray diffraction (XRD), and X-ray photoelectron spectroscopy (XPS) showed that the microbial mats in this region were composed of an electron and X-ray amorphous hydrous ferric oxide (HFO) phase containing 0.6–0.7 mole ratio As:Fe, among the highest As contents observed in naturally occurring HFO's (Morin *et al.*, 2003; Inskeep *et al.*, 2004). Phylogenetic analysis of 16S rDNA cloned from these microbial mat communities suggested that *Hydrogenobaculum, Desulphurella, Acidimicrobium*, and *Meiothermus*-like populations were important organisms inhabiting different microenvironments within the spring (Jackson *et al.*, 2001). In addition, six archaeal 16S rDNA sequences were identified that exhibited poor matches (mean similarity ~90%) to currently known sequences from hydrothermal vents and terrestrial hot springs. Consequently, it was difficult to infer the potential role of these novel organisms in mat development and or geochemical cycling. More generally, direct links between microbial populations and the unique chemical processes occurring in geothermal springs has been limited (Reysenbach & Shock, 2002).

Examination of microbial and geochemical changes occurring during reestablishment of microbial mats following disturbance has served as a useful tool for elucidating the function of individual microbial populations in hot springs (Brock & Brock, 1969; Ferris *et al.*, 1997). For example, Ferris *et al.* (1997) used molecular techniques to assess changes in cyanobacterial populations after microbial mat removal. The apparent physiology and ecological role of specific populations was determined by coupling molecular information with measurements of O_2 production/consumption and $^{14}CO_2$ partitioning over time. In the current study, a similar strategy was used to identify microbial populations associated with geochemical cycling of H_2, S, As, and Fe in an acidic geothermal spring. Specifically, the objectives of this study were to (1) correlate the distribution of bacterial and archaeal sequences in time and space with changes in temperature and geochemical energy gradients occurring throughout the outflow channel of an ASC geothermal spring; (2) identify microorganisms responsible for rapid rates of *in situ* As(III) oxidation; and (3) determine the microorganisms and processes responsible for the formation of As-rich HFO mats. These objectives were addressed by monitoring changes in aqueous and solid phase geochemistry, and 16S rDNA sequence distribution occurring during microbial colonization and mat establishment in a newly formed discharge channel. The suite of complementary analyses included 16S rDNA molecular fingerprinting using denaturing gradient gel electrophoresis (DGGE) and subsequent 16S rDNA sequence analysis, along with a variety of chemical, microscopic, and spectroscopic techniques.

MATERIALS AND METHODS

Site description and sampling procedures

The acid-sulphate-chloride (ASC) geothermal spring selected for this study, referred to as *Succession Spring* (44°43′75.7″ N. Latitude, 110°42′74.7″ W. Longitude), is geochemically typical of many ASC springs found in the Hundred Springs Plain of Norris Geyser Basin, Yellowstone National Park. On July 18, 2001, discharge water from this small spring (source pool approximately 17 cm in diameter and 3 cm deep in the center, flow rate ~7 litre min^{-1}) was redirected into a new channel through coarse-textured siliceous parent material characteristic of Norris Basin. The new channel was approximately 9 cm wide, a maximum of 1 cm deep, and extended approximately 15 m before mixing with runoff from adjacent springs. Immediately after redirecting the flow, a series of glass slides (1 × 4 × 50 mm) was placed in the new channel at distances of 0, 2, 4, 8, and 12 m from the spring source pool to serve as surfaces for growth of microbial mats and deposition of solid phases. Chemical and microbial changes were evaluated at 10 dates from July 18 to October 29, 2001. At each sampling date, two sets of glass slides were removed from the channel, placed in 15 mL sterile tubes, and immediately frozen (placed on dry ice until storage at –80 °C). The slides were subsequently utilized for physical, chemical, and molecular characterization of adhering microbial mats

and solid phases (described below). At the same dates, aqueous samples were collected at 0, 2, 4, 6, 8, 12, and 14 m from the source pool and used for a suite of chemical analyses.

Aqueous phase chemistry

At each sampling date, *in situ* measurements of temperature and temperature-compensated pH were made with a Mettler Toledo MA130 portable pH meter fitted with a Mettler Toledo IP67 NTC electrode and calibrated using pH 1.68 and 4.01 buffers. Samples used for aqueous phase analysis were withdrawn from selected positions in the spring using a 20 mL syringe. Total dissolved sulphide was analysed using the amine-sulphuric acid method (APHA, 1998). Absorbance (664 nm) was measured in the laboratory within 30 h of sampling. Total Fe and Fe(II) in 5 mL filtered (0.22 μm) aliquots were analysed on site using the FerroZine method (To *et al.*, 1999). Absorbance of the FerroZine-Fe(II) complex was measured at 562 nm within 1 h and in most cases within 10 min of sampling. Ion chromatography (IC) was used to determine the concentration of predominant anions (F^-, Cl^-, SO_4^{2-}, NO_3^-, CO_3^{2-}, AsO_4^{3-}) within 1 h and in most cases within 2 min after sample collection [Dionex DX500 Chromatography System, 25 μL injection loop, AS16-4 mm ion exchange column (Dionex Corp., Sunnyvale, CA), eluant gradient of 20–50% 100 mM NaOH]. Total As was also determined with IC using samples pretreated with $KMnO_4$ to oxidize As(III) to As(V). Selected aqueous samples were analysed for Na, K, Ca, Mg, Fe, Si, Al, B, S, P, As, Cd, Cr, Cu, Mn, Ni, Pb, Sb, Se, and Zn using inductively coupled plasma atomic emission spectrometry (ICP-AES). Values for total As determined using ICP were consistently within 10% of values measured with IC. Dissolved organic C (DOC) was measured with a DC-80 carbon analyser (Tekmar-Dohrmann, Cincinnati, OH) after acidifying to 70 mM H_3PO_4 and purging with O_2 for 5 min to remove dissolved carbonate species. Colorimetric analysis of NH_4-N was performed with a Lachat QuickChem FIA+ auto analyser (Zellweger Analytics, Milwaukee, WI). Aqueous H_2 was measured within 18 h after completely filling 72 mL serum bottles with source water and capping. Prior to analysis, serum bottles (stored at 4 °C) were brought to room temperature (21 °C) and a known volume of liquid was removed and replaced with an equal volume of N_2(g). After the sample was shaken for 40 min, 1 mL of headspace was removed and injected into a Carle Series 100 AGC gas chromatograph (Carle Chromatography, Tulsa, OK) equipped with a molecular sieve 13X 80/100 column and thermal conductivity detector (carrier gas: argon @ 30 mL min^{-1}, 50 °C). Concentrations of dissolved H_2 were calculated using a Henry's law constant of 7.5×10^{-4} M atm^{-1} derived from ΔG°_{rxn} values (Amend & Shock, 2001). Dissolved O_2 was measured on site using a FOXY system (USB2000-FL, USB-LS-450, FOXY-R fibre optic probe, Ocean Optics, Inc., Dunedin, FL) with temperature compensation.

Characterization of solid phases

Microbial mats and solid phases deposited on the glass slides were examined with a JEOL 6100 scanning electron microscope (SEM) equipped with an energy-dispersive X-ray spectrometer (EDS) within 22 h of sample collection (incident electron beam = 19 keV). The glass slides were placed on Al-stubs and coated with Au prior to analysis under a cryostage to retain microbial cell integrity. Total elemental composition of selected mat/solid phase samples was determined using a four acid heat treatment followed by elemental analysis with ICP-AES. The mineralogy of several samples was evaluated using homogeneous composites of microbial mat solid phase. X-ray diffraction (XRD), X-ray absorption near edge spectroscopy (XANES), and extended X-ray absorption fine structure spectroscopy (EXAFS) data were collected at the Stanford Synchrotron Radiation Laboratory in collaboration with Drs S. Fendorf and B. Bostick (Inskeep *et al.*, 2004). The amount of oxalate-extractable Fe was determined by extracting 0.1 g solid phase in 30 mL of 0.175 M NH_4-oxalate/0.1 M oxalic acid at pH 3 in the dark for 2 h (Loeppert & Inskeep, 1996).

Thermodynamic calculations

Microorganisms residing in the ASC springs of Norris Basin can, in theory, derive energy from a wide variety of inorganic chemical reactions. The free energies (ΔG_{rxn}, kJ mol^{-1}) of several potentially important redox couples were calculated using the familiar expression:

$$\Delta G_{rxn} = \Delta G^\circ_{rxn} + RT \ln(Q_{rxn}) \quad (1)$$

where standard state free energies of reaction (ΔG°_{rxn}) as a function of temperature were obtained from Amend & Shock (2001), and temperature corrected activities of chemical species used in the reaction quotient (Q_{rxn}) were calculated with the aqueous equilibrium model, Visual MINTEQ (Allison *et al.*, 1991), using measured values of chemical constituents at the spring source. Values of ΔG°_{rxn} not available in the literature were calculated using temperature corrected standard free energies of formation (ΔG°_f) for constituents measured in the spring (Amend & Shock, 2001). Temperature corrected values of ΔG°_{rxn} and ΔG°_f were provided at specific temperatures by Amend & Shock (2001, e.g. 45, 55, 70, and 85 °C), and the values at 70 °C (within 8 °C of the source) were used for calculations of ΔG_{rxn}. This approximation resulted in deviations to ΔG_{rxn} that were no greater than 3 kJ mol^{-1} compared to fitted values of ΔG°_{rxn} and ΔG°_f that corresponded to temperatures measured at the source (78 °C). Visual MINTEQ was also used to estimate saturation indices [log (ion activity product (IAP)/solubility product (Ksp))] for various solid phases at

spring temperatures. Solubility constants for As_2S_3 (orpiment) and As_2S_3 (amorphous) were based on constants derived from Eary (1992) and Webster (1990) and further adopted by Nordstrom & Archer (2003). Important equilibrium reactions and aqueous species used for calculating saturation indices of As_2S_3 phases were:

$$As_2S_3(s) + 6H_2O = 2H_3AsO_3(aq) + 3HS^- + 3H^+$$
$$\log K_{(orp,\,25\,^\circ C)} = -46.3, \quad \log K_{(am,\,25\,^\circ C)} = -44.9 \qquad (2)$$

$$3H_3AsO_3(aq) + 6HS^- + 5H^+ = H_2As_3S_6^- + 9H_2O$$
$$\log K = 72.3_{(25\,^\circ C)}, \quad \Delta H^\circ_{rxn} = -343.8 \text{ KJ mol}^{-1} \qquad (3)$$

The reaction enthalpy (ΔH°_{rxn}) for the formation of $H_2As_3S_6^-$ (Eqn 3) was estimated using the van't Hoff expression and equilibrium constants determined at temperatures ranging from 25 to 90 °C (Eary, 1992; Amend & Shock, 2001; Nordstrom & Archer, 2003). The $AsS(OH)(SH)^-$ complex, which has been shown to be important in As(III)-sulphide solutions (Helz *et al.*, 1995), was also included in the equilibrium calculations.

Molecular analysis of microbial communities

Total DNA was extracted from microbial mats formed on glass slides and from sand adjacent to the stream using the FastDNA SPIN Kit for Soil (Bio 101, Vista, CA). Polymerase chain reactions (PCR) using the total DNA extracts targeted specific regions within the 16S rRNA gene of the domains bacteria and archaea. One primer set was designed to capture a 322 bp segment within the domain bacteria using Bac1070 forward (*E. coli* positions 1055–1070) paired with Univ1392 reverse-GC (*E. coli* positions 1392–1406; Jackson *et al.*, 2001). To facilitate analysis by denaturing gradient gel electrophoresis (DGGE), the reverse primer incorporated a 40 bp GC-rich clamp (Ferris *et al.*, 1996). A second primer set was designed to capture a 461 bp region within the domain Archaea, utilizing the forward primer Arc931f, and the reverse primer Univ1392 reverse-GC as described above (Jackson *et al.*, 2001). The 50 μL PCR mixtures contained 10 mM Tris-HCl (pH 8), 50 mM KCl, 0.1% Triton X-100, 4.0 mM $MgCl_2$, 800 μM dNTP's, 0.5 μM of each primer, 1.25 U *Taq* DNA polymerase (Promega, Madison, WI), and 1–5 μL template DNA (2–20 ng). Thermal cycler protocol was 94 °C for 4 min, 25–35 cycles of 94 °C, 54 °C and 72 °C each for 55 s, and a final 7 min extension period at 72 °C. Negative control reactions (no template) were routinely performed to ensure purity.

Denaturing gradient gel electrophoresis (DGGE) was used to separate 16S rRNA gene fragments following a method modified from Ferris *et al.* (1996). PCR products (~90 ng per lane) were loaded onto gels consisting of 8% acrylamide and a 40–70% denaturing gradient of urea/formamide. The gels were electrophoresed at 60 V at 60 °C for 17 h using a DCode System (Bio-Rad, Hercules, CA) and stained with SYBR Green II (Molecular Probes, Eugene, OR) for 30 min prior to photography using UV transillumination. DGGE bands were purified by stabbing with a sterile pipet tip and rinsing the tip in molecular biology grade water, which was then used as template for PCR. The position and purity of PCR amplified band stabs were checked using DGGE, and if necessary, the process was repeated until pure bands were obtained. Prior to sequencing, DNA was purified using a Microcon PCR centrifugal filter kit (Millipore Corp. Bedford, MA). Bands were sequenced by PCR amplification using primers 1070 forward for bacteria and 931 forward for archaea and 1392 reverse (without the GC clamp). The sequencing reaction was performed using an ABI Prism BigDye Terminator Cycle Sequencing Ready Reaction Kit (Perkin-Elmer, Foster City, CA) and the samples were processed on an ABI Prism 310 capillary sequencer (Perkin-Elmer). Sequencher 3.1.1 software (Gene Codes Corporation, Ann Arbor, MI) was used to align and edit the resultant sequences that were then compared with sequences found in the GenBank database using BLAST (Altschul *et al.*, 1997).

RESULTS AND DISCUSSION

Aqueous temperature and geochemistry

Temperature values declined exponentially with distance down gradient, averaging 79.2 °C at the source and 48.3 °C at 14 m. Temperatures varied approximately 5–10 °C at any given distance down the outflow channel (Fig. 1A), due to both fluctuations in source water temperature and variation in spring discharge rates. Although discharge rates were generally consistent over short time-frames (days-weeks), they varied from approximately 5 L min^{-1} on day 14 to a maximum of 9 L min^{-1} on day 103. The variation in flow rates observed in this study is consistent with seasonal variation in geothermal discharge rates from most springs in Norris Basin (personal comm., Dr Irving Friedman; http://volcanoes.usgs.gov/yvo/hydro.html). The pH values were relatively consistent over the sampling period but showed a slight decline down gradient, where pH values averaged 3.10 ± 0.07 at the source and decreased to 2.97 ± 0.08 by 14 m. The decline in pH may be due primarily to evaporation (D. K. Nordstrom, personal comm.). Concentrations of selected chemical constituents (Table 1) measured in the source water of *Succession Spring* yield a computed ionic strength (Visual MINTEQ) of 16.5 mM, comprised primarily of Na^+, H^+, Cl^-, SO_4^{2-}, K^+ and dissolved inorganic carbon (DIC).

Aqueous chemistry of arsenic

The total soluble As (As_{TS}) concentration at the source ranged from 70 to 90 μM, considerably higher (~3 times) than adjacent springs in Norris Basin that have been the

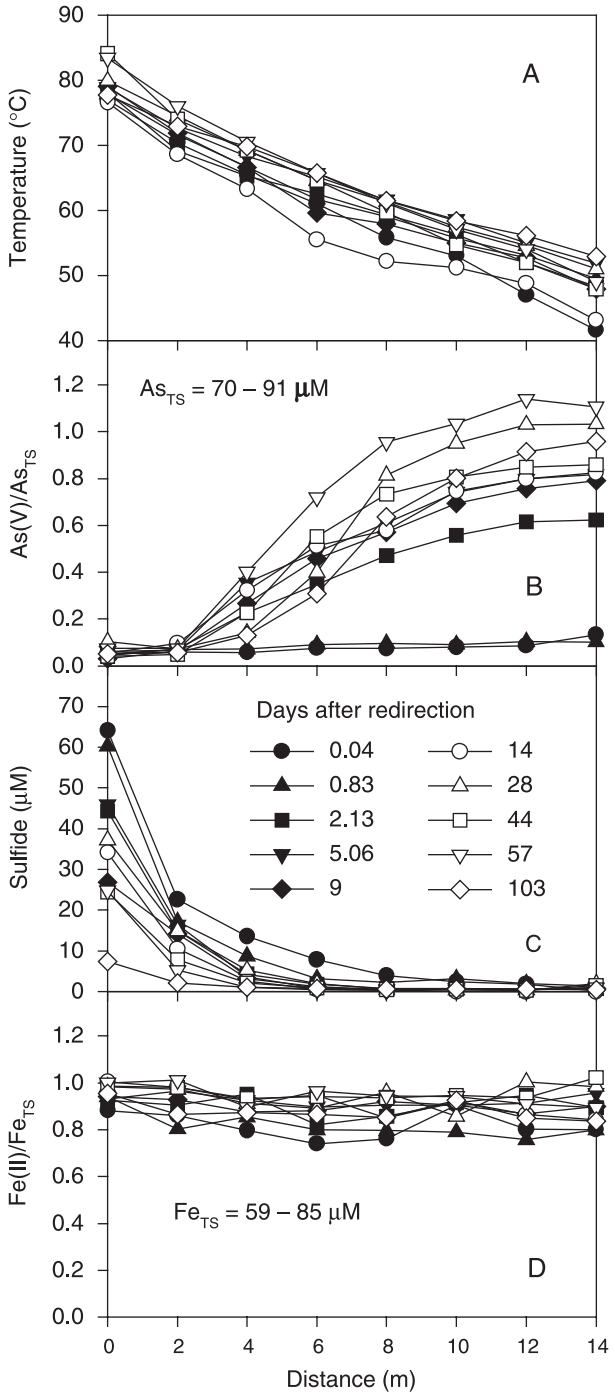

Fig. 1 Changes in aqueous temperature and selected aqueous geochemical constituents as a function of distance from spring discharge measured at different sampling dates after spring redirection [As(V) and Fe(II) are shown as a ratio of these valence states to total soluble (TS) concentrations and sulphide represents total dissolved sulphide, primarily H_2S(aq) at pH = 3].

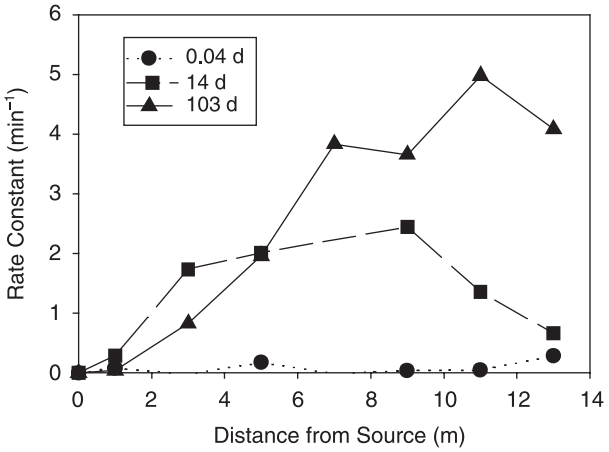

Fig. 2 Pseudo first-order rate constants (k) for the oxidation of As(III) calculated based on measured values of As(III) and As(V) as a function of distance from spring discharge at three sampling dates.

subject of recent geochemical investigations (Langner *et al.*, 2001; Inskeep *et al.*, 2004). Thermodynamic calculations using temperature corrected constants in Visual MINTEQ, predicted that the source water (2 d, 78.1 °C) was significantly undersaturated with respect to amorphous As_2S_3 and orpiment [log (IAP/Ksp) for As_2S_3(am) = –3.3 and As_2S_3(orp) = –2.4]. Arsenite was the predominant valence of As in *Succession Spring* source water [nearly 100% As(III)] and no signs of As(III) oxidation were observed from 0 to 14 m down gradient of the source during the first two sampling times (0.04 and 0.83 d; Fig. 1B). After 2 days, however, significant oxidation of As(III) to As(V) was detected, and by 14 m down gradient, 62% of the total As was present as As(V). The fraction of As(III) oxidized continued to increase during the study, and by day 57, 100% of the initial As(III) was oxidized by 12 m. Apparent *in situ* first-order rate constants ($k = \ln[As_{x1}/As_{x2}]\ t^{-1}$) for the oxidation of As(III) were determined at each sampling date using incremental As(III) concentrations at paired distances (e.g. $x_1 = 0$ and $x_2 = 2$ m, etc.) along the outflow channel, and measured travel times between the paired distances. Average residence times for the total spring interval from 0 to 14 m were only ~1 minute. The calculated As(III) oxidation rate constants increased from ~0.08 min^{-1} at the first sampling time ($t_{1/2}$ ~9 min) to 4–5 min^{-1} by 103 days ($t_{1/2}$ ~0.15 min; Fig. 2). At 14 days, As(III) oxidation rate constants level off between 3 and 9 m. However, As(III) oxidation rate constants from 7 to 13 m increased significantly at 103 days (Fig. 2), corresponding to formation of a highly developed HFO mat observed from 3 to 14 m (Fig. 3; described below). The As(III) oxidation rates observed in this study were considerably faster than rates observed in other thermal and nonthermal environments, including other acid and alkaline thermal springs in YNP ($t_{1/2}$ = 0.6 min, Langner *et al.*, 2001; $t_{1/2}$ = 1.2 min, Gihring *et al.*, 2001) and macrophyte communities in streams receiving geothermal discharge ($t_{1/2}$ = 20 min, Wilkie & Hering, 1998). Importantly, As(III) oxidation occurred over distances of 2–12 m, representing a wide range of temperature and geochemical

Table 1 Concentrations of selected chemical constituents measured in *Succession Spring* source water on day 103 (October 29, 2001)

Cations and Anions	Concentration (μM)	Weak Acids/ Bases	Concentration (μM)
Na^+	12 532	Si	4819
K^+	954	DIC†	1763
Ca	116.7	B	651
Al	108.7	As	70.1
Fe	86.1	NH_4^+	44.9
Mg	9.4	DOC‡	41.0
Zn	2.1	S(–II)	7.4
Mn	0.65	P	0.9
Cl^-	13 342	$H_2(aq)$§	0.036 (0.028)
SO_4^{2-}	1331	$O_2(aq)$§	<0.08 (0.00)
F^-	174.9	Charge Difference¶	3.0%
NO_3^-	24.4	Ionic Strength¶	0.0165 M

*Undetected elements with method detection limits in parenthesis: Se (<4 μM); Ni (<0.9 μM); Sb, Pb, Cr (<0.6 μM); Cd, Cu (<0.2 μM). †Dissolved inorganic C. ‡Dissolved organic C. §Means and standard deviations of $H_2(aq)$ and $O_2(aq)$ concentrations measured on 11-26-02, 7-14-03, and 10-28-03. ¶Charge difference and ionic strength calculated using Visual MINTEQ (Allison *et al.*, 1991).

conditions, suggesting that several different microorganisms contributed to As(III) oxidation during microbial colonization.

Profiles of dissolved H_2S

Concentrations of dissolved sulphide decreased to detection limits of approximately 2 μM after 10 m at all sampling events (Fig. 1C). Apparent first-order rate constants for the disappearance of $H_2S(aq)$ ranged from 0.8 to 12 min^{-1} (corresponding to $t_{1/2}$ of 0.9–0.06 min) with maximum rate constants found near the source. Despite fluctuating sulphide concentrations at the spring source ranging from 8 to 64 μM, no changes in the $H_2S(aq)$ disappearance profiles were observed prior to or during microbial mat formation, suggesting that abiotic pathways including degassing of $H_2S(aq)$ and or oxidation to S° and thiosulphate upon oxygenation (Xu *et al.*, 1998) make important contributions to the disappearance of dissolved sulphide. Further, under acidic conditions, thiosulphate rapidly disproportionates to S° and sulfite, and sulfite, in turn, oxidizes rapidly to sulphate (Xu *et al.*, 1998). The lack of detectable thiosulphate and sulfite using ion chromatography (IC) may be explained by the transient nature of these compounds at this pH (~3.0). The rapid abiotic oxidation of $H_2S(aq)$ is consistent with S° depositional patterns as a function of time and distance (discussed below). In addition, the possible oxidation of H_2S to SO_4^{2-} could not be quantified due to the high background levels of SO_4^{2-} (~1.3 mM) relative to H_2S (<0.07 mM).

Disappearance of dissolved inorganic C

Concentrations of DIC measured in the source water ranged from 1.0 to 2.3 mM over the study period. As with $H_2S(aq)$ (Fig. 1C), a rapid decline in DIC as a function of distance from the source was observed, typically decreasing to <0.1 mM (detection limit) by 12 m. The rapid decline in $H_2CO_3^*(aq)$ with distance (data not shown) was attributed primarily to

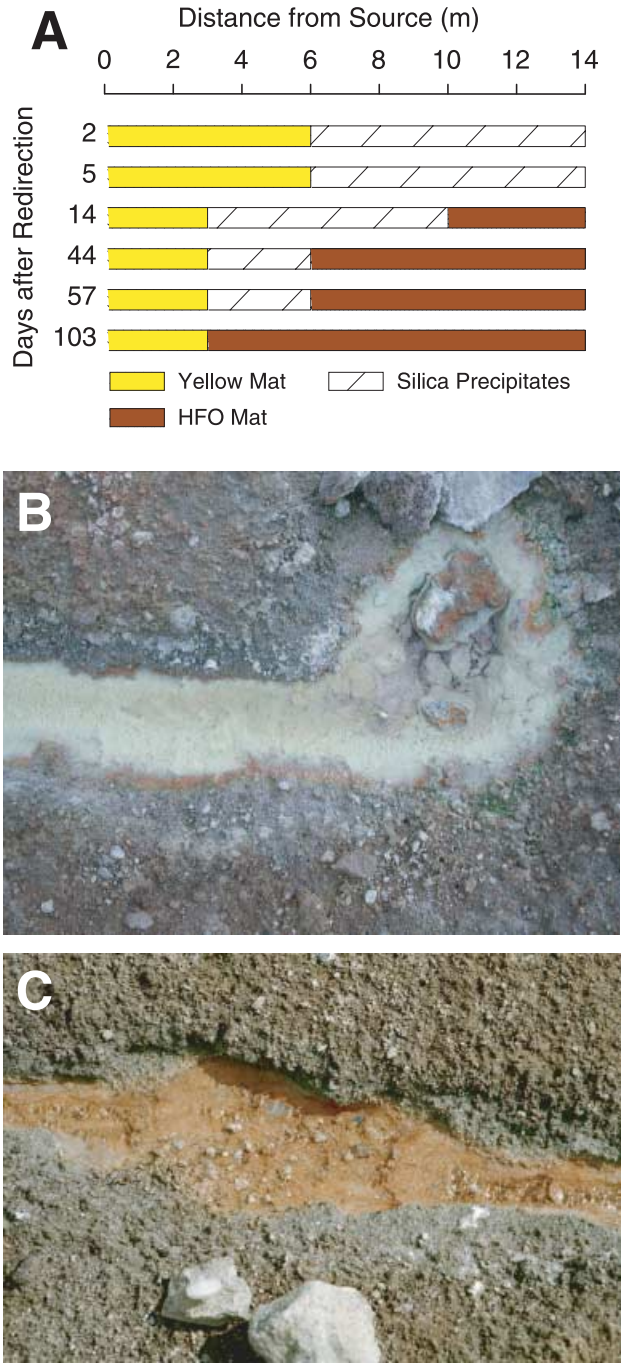

Fig. 3 Chronological progression of elemental S° (yellow mat), hydrous ferric oxide (HFO), and silica deposition as a function of distance from spring discharge (A). Example photographs of *Succession Spring* are shown 57 days after flow redirection (September 13, 2001) documenting elemental S° deposition near and immediately down gradient of spring discharge (0–1 m) (B), and deposition of As(V)-hydrous ferric oxide (HFO) microbial mats at 7–9 m from spring discharge (C).

degassing of CO_2(aq). The source waters were more than 100 times oversaturated with respect to atmospheric pCO_2(g), consequently, there was a significant disequilibrium that drives degassing, especially at pH 3 where $H_2CO_3^\circ$ is the predominant carbonate species. Fixation of CO_2 via autotrophic organisms is another potential sink for CO_2, although first-order fits of the data did not show any trends or changes in rate constants that would be attributable to the time course of microbial mat development (data not shown). Given the high concentrations of DIC within the upper portion (0–8 m) of the stream channel, autotrophic organisms are not likely limited by the availability of CO_2(aq).

Soluble Fe, O_2 and H_2 profiles

Concentrations of total soluble Fe (Fe_{TS}) at discharge (0 m) varied from 59 to 86 μM during the study (Fig. 1D), and no consistent losses (greater than 10%) of Fe_{TS} were observed down gradient. Furthermore, the predominant valence of Fe was Fe(II), comprising ~80–100% of the Fe_{TS} over the course of the study. No consistent changes in Fe(II):Fe(III) ratios were noted as a function of time or distance down gradient. As expected, rapid in-gassing of O_2 occurred with distance. Concentrations of dissolved O_2 have been measured several times since the original study in 2001; wherein values have been consistently below detection limits at the source (<0.08 μM), but increased to predicted saturation levels by 12 m (measured values at 12 m ranged from 144 to 150 μM; predicted saturation @ 55 °C and 2195 m elevation = 144 μM). Finally, H_2(aq) concentrations have also been measured several times since the original study and found to range from 15 to 100 nM (mean = 36 nM) at the source, consistent with H_2(aq) levels measured in other ASC springs in Norris Basin (G. Ackerman, unpublished data; Spear & Pace, 2004).

Table 2 Predicted Gibbs free energies (ΔG_{rxn}) for reactions potentially used by chemolithotrophic organisms at the source of *Succession Spring*. All calculations were based on temperature corrected equilibrium constants and predicted activities of constituents (Visual MINTEQ) measured at 0 m on day 103*

	Reaction†	ΔG_{rxn} (kJ mol electron^{-1})
1	$H_2(aq) + 0.5O_2(aq) = H_2O$	–94
2	$H_2(aq) + 0.25NO_3^- + 0.5H^+ = 0.25NH_4^+ + 0.75H_2O$	–64
3	$H_2(aq) + 2Fe^{3+} = 2Fe^{2+} + 2H^+$	–63
4	$H_2(aq) + H_2AsO_4^- + H^+ = H_3AsO_3^\circ + H_2O$	–33
5	$H_2(aq) + S^\circ = H_2S(aq)$	–16
6	$H_2(aq) + 0.25SO_4^{2-} + 0.5H^+ = 0.25H_2S(aq) + H_2O$	–11
7	$H_2S(aq) + 2O_2(aq) = SO_4^{2-} + 2H^+$	–84
8	$H_2S(aq) + 0.5O_2(aq) = S^\circ + H_2O$	–78
9	$H_2S(aq) + 2Fe^{3+} = 2Fe^{2+} + 2H^+ + S^\circ$	–46
10	$H_2S(aq) + H_2AsO_4^- + H^+ = H_3AsO_3^\circ + S^\circ + H_2O$	–17
11	$H_2S(aq) + 0.25NO_3^- = 0.25NH_4^+ + S^\circ + 0.375O_2 + H^+$	–14
12	$S^\circ + 1.5O_2(aq) + H_2O = SO_4^{2-} + 2H^+$	–85
13	$S^\circ + 0.75NO_3^- + H_2O + 2H^+ = SO_4^{2-} + 0.75NH_4^+$	–76
14	$S^\circ + 6Fe^{3+} + 4H_2O = 6Fe^{2+} + SO_4^{2-} + 8H^+$	–54
15	$S^\circ + 6\,Fe(OH)_3(s) + 10H^+ = 6Fe^{2+} + SO_4^{2-} + 14H_2O$	–54
16	$S^\circ + 3H_2AsO_4^- + H^+ + H_2O = 3H_3AsO_3^\circ + SO_4^{2-}$	–24
17	$H_3AsO_3^\circ + 0.5O_2(aq) = H_2AsO_4^- + H^+$	–61
18	$H_3AsO_3^\circ + 0.25NO_3^- + 0.25H_2O = H_2AsO_4^- + 0.5H^+ + 0.25NH_4^+$	–30
19	$H_3AsO_3^\circ + 2Fe^{3+} + H_2O = H_2AsO_4^- + 2Fe^{2+} + 3H^+$	–29
20	$H_3AsO_3^\circ + 2Fe(OH)_3(s) + 3H^+ = H_2AsO_4^- + 2Fe^{2+} + 5H_2O$	–28
21	$Fe^{2+} + 0.25O_2(aq) + H^+ = Fe^{3+} + 0.5H_2O$	–32
22	$Fe^{2+} + 0.25O_2(aq) + 2.5H_2O = Fe(OH)_3(s) + 2H^+$	–32
23	$Fe^{2+} + 0.125NO_3^- + 1.25H^+ = Fe^{3+} + 0.125NH_4^+ + 0.375H_2O$	–1
24	$Fe^{2+} + 0.125NO_3^- + 2.625H_2O = Fe(OH)_3(s) + 0.125NH_4^+ + 1.75H^+$	–1
25	$NH_4^+ + 2O_2(aq) = NO_3^- + 2H^+ + H_2O$	–28

*H_2 and O_2 concentrations used in these calculations [O_2(aq) = 80 nM (detection limit), H_2(aq) = 36 nM] are means of measurements made on 11-26-02, 7-14-03, and 10-28-03. †Reactions written in terms of predominant species at spring conditions.

Energetics and chemolithotrophy

The waters and associated solid phases of *Succession Spring* contain H_2, H_2S, S°, Fe(II), As(III), and NH_4^+ that may serve as important electron donors driving primary production. In addition, S°, SO_4^{2-}, NO_3^-, Fe(III), As(V) and O_2 were present at significant concentrations at various distances down the outflow channel, and may be important electron acceptors for respiration. Combinations of these electron donors and acceptors can serve to drive energy conserving reactions for a diversity of thermophilic microorganisms (Amend & Shock, 2001). To assess the chemical energy available to microorganisms, the Gibbs free energies (ΔG_{rxn}) for selected oxidation-reduction reactions were predicted using temperature-corrected thermodynamic equilibrium constants in conjunction with predicted activities (MINTEQ, Allison *et al.*, 1991) of constituents measured at the source (Table 2). The redox couples summarized in Table 2 are all exergonic under these conditions and represent likely candidates for microbial metabolism based on the geochemical attributes of ASC springs. It is possible that organisms utilizing reactions with the greatest energy yields may have a competitive advantage, at least based on thermodynamic favourability. With O_2 as an electron acceptor, the energy available per mole of electron transferred was greatest for H_2 (Rxn. 1 in Table 2, ΔG_{rxn} = –94 kJ mol electron^{-1}) followed in order by S° (oxidation to SO_4^{2-}), H_2S (oxidation to S°), As(III), Fe(II), and NH_4^+ (oxidation to NO_3^-). Although complete oxidation of H_2S(aq) to SO_4^{2-} is significantly exergonic (Rxn. 7, –84 kJ mol electron^{-1}), microbial pathways for this 8 e^- transfer are not well documented (Madigan *et al.*, 2002). As expected, for any given electron donor (i.e. H_2, S°, H_2S, As[III], and Fe[II]), the amount of energy available decreases as O_2 is replaced as an electron acceptor with species such as NO_3^- or Fe(III) (Table 2). Consequently, organisms capable of utilizing H_2, H_2S or S° coupled with O_2 as an

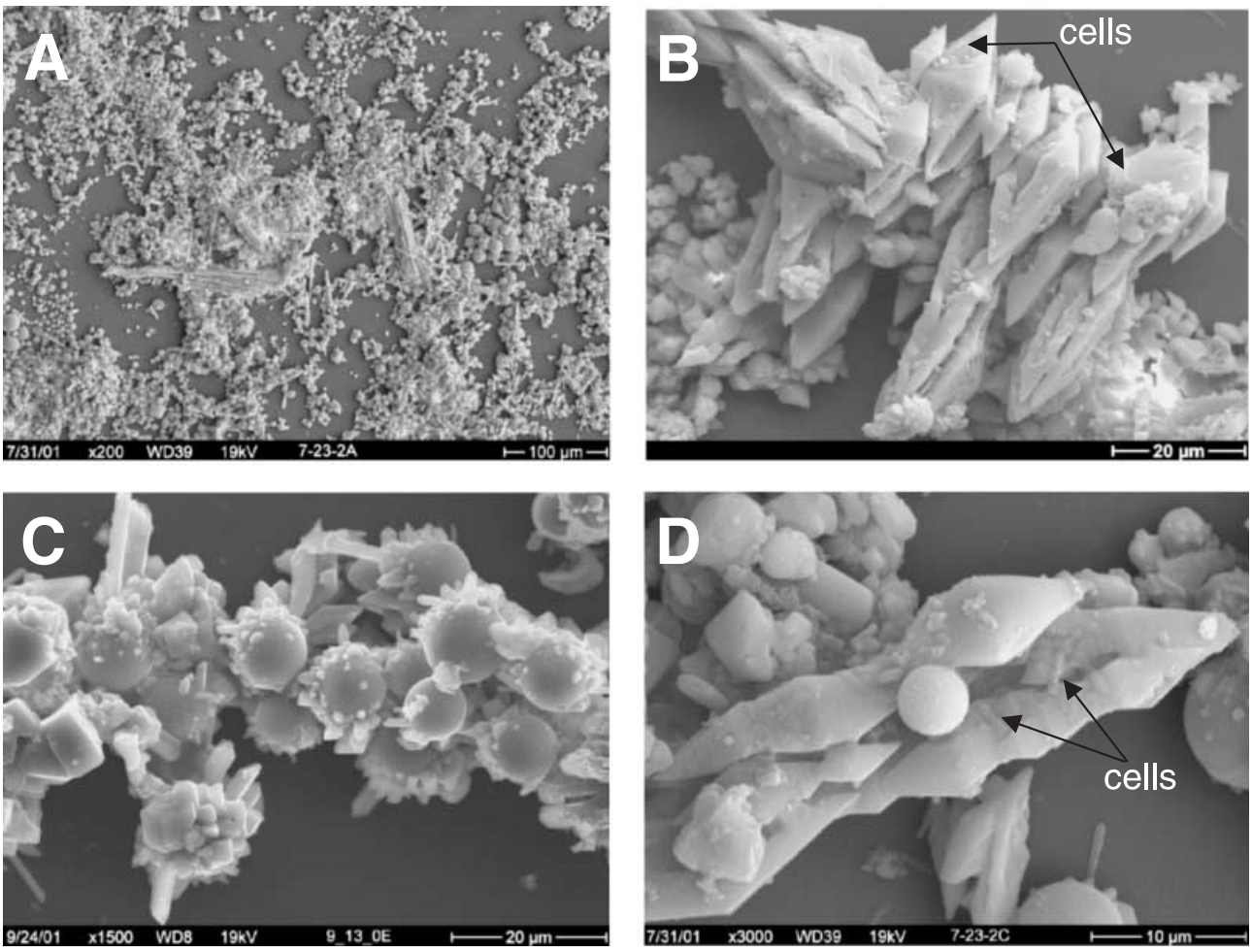

Fig. 4 Scanning electron micrographs (SEM) of elemental S° deposited at 2 m from spring discharge. The low magnification (200X) image (A) reveals S° spheres of variable diameters and rhombohedral chains deposited during the first 5 days after spring redirection. Higher magnification images of S° rhombs and spheres (panels B, D) reveal the presence of microbial cells (rods and filaments) colonizing S° surfaces. In many cases, S° spheres appear to serve as possible nucleation sites for rhombohedral formation (panel C).

electron acceptor would be expected to have a competitive advantage near the source of ASC springs.

Temporally and spatially linked geochemical transformations and microbial community development

One of the primary goals of this study was to describe the distribution of microorganisms as a function of geochemical and thermal gradients. Towards this end, visible and microscopic observations of solid phase deposition and microbial mat development were coupled with corresponding changes in aqueous chemistry and 16S rDNA sequence distribution occurring after spring redirection. Fingerprints of microbial communities located at five positions in the stream channel were obtained at seven sampling dates using PCR amplification and denaturing gradient gel electrophoresis (DGGE) of 16S rDNA fragments.

Deposition of elemental S

The first obvious change in solid phase deposition and microbial community development occurred within 2 days, when yellow solid phase began to line the channel floor from 0 to 6 m (Fig. 3). Electron micrographs and elemental analysis (EDAX) of the yellow solid phase revealed several types of S° (>92 atom percentage S) morphologies including spheres and rhombohedral crystals (Fig. 4). In some cases, the S° spheres appear to serve as nucleation sites for growth of orthorhombic crystals (Fig. 4C). Spheres and rhombs of S° have been previously reported in geothermal springs (Kostov & Kostov, 1999). Electron micrographs also demonstrated evidence of initial stages of microbial colonization by day 2 where rods and filaments (~0.7 µm diameter) were observed on orthorhombic S° surfaces. The role of these early colonizers in formation and deposition of the S° phase was not clear, given that the

majority of S° phases did not reveal any surface-attached microorganisms corresponding to the time frame necessary to deposit this phase. Rather, the rapid deposition of elemental S° was attributed primarily to O_2(g) in-gassing followed by kinetically favoured abiotic oxidation of H_2S to S° (Xu *et al.*, 1998). The length of the S° depositional zone gradually decreased during the course of the study and retreated to 3 m by day 14 (Fig. 3). The decrease in length of the yellow mat correlated with a corresponding decline in source water H_2S(aq) concentrations (Fig. 1C). During the study period, concentrations of H_2S(aq) at the lower boundary of the S° zone were consistently between ~0.5–2 μM, suggesting that concentrations >2 μM are required to effectively support the formation of S° at these temperatures. The corresponding temperature range defining the S° depositional zone was approximately 60–84 °C (Fig. 1A and 3).

Colonization by *Hydrogenobaculum*-like organisms: links to H_2, S° and As(III)

The first microorganisms to colonize the stream channel after spring redirection were closely related to *Hydrogenobaculum* sp. strain NOR3L3B (>98% similarity; Eder & Huber, 2002). Three different *Hydrogenobaculum* sequence types (B4, B5, and B182) were observed within 1–2 days at positions 2, 4, or 8 m (Fig. 5, Table 3). With time, *Hydrogenobaculum*-like sequences were detected at all sampling positions (0–12 m) in the stream, representing the only genus that was so widely distributed across thermal and geochemical gradients (Fig. 5). The sequence of a possible hyperthermophilic population, designated B23, was detected on day 103 at 0–2 m, a location characterized as anaerobic to microaerobic and containing significant levels of H_2 and H_2S. Another population represented by band B156 was detected only at 4 m, possibly a function of reduced thermal or H_2S tolerance, or dependence on higher O_2. The population corresponding to sequence B4 was detected at positions from 2 to 12 m. It is possible that the *Hydrogenobaculum*-like populations detected at the lower positions of the stream channel (B4 and B182) were adapted to more aerobic conditions and lower levels of H_2 and H_2S. The detection of different but highly related *Hydrogenobaculum*-like sequences (>98% similarity to each other; Table 3) across the thermal and geochemical gradients of the stream channel suggested that these populations may be adapted to different microenvironments. The presence of different *Hydrogenobaculum*-like sequences was also observed in *Dragon Spring*, where molecular analysis revealed 16 different populations (operational taxonomic units using RFLP analysis) at two sampling locations (Jackson *et al.*, 2001).

The *Hydrogenobaculum*-like populations detected in this study were all close relatives of known *Hydrogenobaculum sp.* including *Hydrogenobaculum sp.* strain NOR3L3B (> 98% similarity; Eder & Huber, 2002), cultivated from a 91 °C spring in Norris Basin, *H. acidophilium*, isolated from a solfatara in Japan

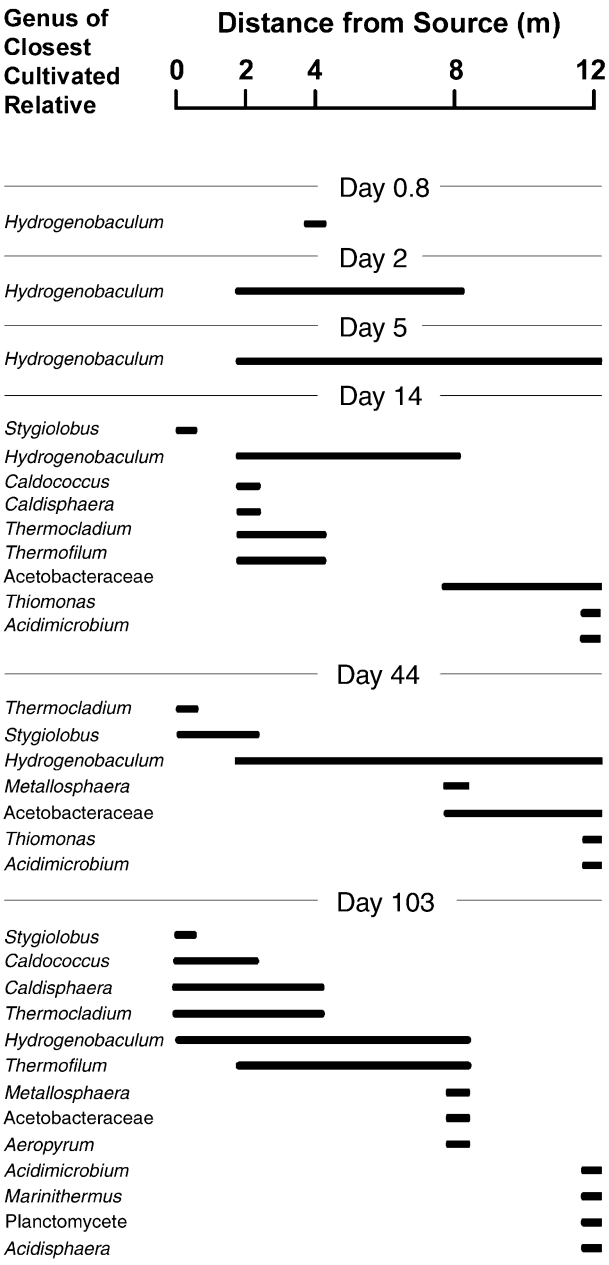

Fig. 5 Appearance of 16S rDNA sequences (as represented by their closest cultivated relatives, GenBank) as a function of distance within the outflow channel from 0.8 through 103 days. Additional information regarding percent similarity of the detected sequences to these relatives is provided in Table 3. In some cases, an entry here refers to several closely related sequences of the same genus. The data presented here are based on results from denaturing gradient gels (40–70%) of 16S rDNA fragments obtained by extracting and amplifying DNA using universal bacterial primers (1070f and 1392r) and universal archael primers (931f and 1392r).

(>97% similarity; accession no. D16296; Shima & Suzuki, 1993), and *Hydrogenobaculum sp.* strain H55 isolated from *Dragon Spring* (>97% similarity; accession no. AY268103; Donahoe-Christiansen *et al.*, 2004). These organisms are all thermoacidophilic, autotrophic microaerobes that utilize H_2 as an energy

Table 3 Accession numbers for partial 16S rDNA sequences obtained from *Succession Spring* and, percent sequence similarity and characteristics of the nearest cultivated GenBank neighbours*

		Nearest Cultured GenBank neighbour*			
Accession Number	DGGE Band Number	Percent Similarity	Cultural Organism	Phylogenetic Group	Characteristics of Cultured Organisms
AY191870	B23	98.6	*Hydrogenobaculum* sp. NOR3L3B	*Aquificales*	microaerophilic, chemolithotrophic, H_2-oxidizer
AY191871	B5	99.1	*Hydrogenobaculum* sp. NOR3L3B	*Aquificales*	
AY191873	B156	99.6	*Hydrogenobaculum* sp. NOR3L3B	*Aquificales*	
AY191869	B4	99.5	*Hydrogenobaculum* sp. NOR3L3B	*Aquificales*	
AY191874	B182	99.5	*Hydrogenobaculum* sp. NOR3L3B	*Aquificales*	
AY191883	B22	98.3	*Stygiolobus azoricus*	*Crenarchaeota*	obligately anaerobic, chemolithotrophic H_2-oxidizer, S-reducer
AY191887	B168	96	*Stygiolobus azoricus*	*Crenarchaeota*	
AY191882	B21	97.7	*Stygiolobus azoricus*	*Crenarchaeota*	
AY191881	B19	97.6	*Caldococcus noboribetus*	*Crenarchaeota*	anaerobic, heterotrophic S-reducer
AY191885	B82	97.6	*Caldococcus noboribetus*	*Crenarchaeota*	
AY191890	B185	95.8	*Caldisphaera lagunensis*	*Crenarchaeota*	anaerobic, heterotrophic, S-reducer
AY191886	B88	98.6	*Thermocladium modestius*	*Crenarchaeota*	anaerobic-microaerophilic obligately heterotrophic, S-reducer
AY191879	B10	98.1	*Thiomonas* sp. Ynys3	β *Proteobacteria*	aerobic, Fe-oxidizer, S_2O_3-oxidizer
AY191899	BG39	98.5	*Acidimicrobium* sp. Y0018	*Actinobacteria*	aerobic-anaerobic, Fe(II)-oxidizer, Fe(III)-reducer
AY191884	B25	98.1	*Metallosphaera prunae*	*Crenarchaeota*	obligate aerobe, S-oxidizer
AY191880	B14	99.1	Acetobacteraceae Y008	α *Proteobacteria*	heterotrophic, Fe(III)-reducer
AY191888	B179	96.7	*Acidisphaera rubrifaciens*	α *Proteobacteria*	aerobic, heterotrophic, contains bacteriochlorophyll
AY191892	BG2	89.3	*Thermofilum pendens*	*Crenarchaeota*	anaerobic, S-reducer
AY191894	BG11	89.1	*Aeropyrum pernix* OH1	*Crenarchaeota*	aerobic, heterotrophic
AY191889	BG6	90.7	*Marinithermus hydrothermalis*	*Deinococcus-Thermus*	obligately aerobic, heterotrophic
AY191895	BG12	92.3	*Planctomycete strain 567*	*Planctomycete*	nonthermophilic

*The nearest GenBank neighbour was determined by comparing partial 16S rDNA sequences of DGGE bands to sequences in the GenBank database using BLAST (Altschul *et al.*, 1997).

source. In addition, *H. acidophilium* requires S° for growth. Furthermore, strain H55 has been shown to oxidize As(III), apparently for detoxification purposes (Donahoe-Christiansen *et al.*, 2004). Indeed, the oxidation of As(III) to As(V) from 2 to 8 m was initially detected 2 days after spring redirection (Fig. 1B), and correlated with the appearance of three *Hydrogenobaculum*-like populations (bands B4, B5, and B182; Fig. 5). By 14 d, *in situ* As(III) oxidation rates were significant from 3 to 9 m (Fig. 2), attributable primarily to the early colonization by *Hydrogenobaculum*-like populations.

The fact that As(III) oxidation was not observed between 0 and 2 m may be explained by H_2S inhibition of As(III) oxidation by *Hydrogenobaculum* populations (Donahoe-Christiansen *et al.*, 2004).

Appearance of possible hyperthermophiles at 0–2 m: links to H_2 and S°

The source waters of *Succession Spring* are considerably warmer than geochemically similar adjacent ASC springs, and ranged from 77 to 84 °C during this study. Microorganisms growing optimally above 80 °C are considered hyperthermophiles and currently, there is limited information about the distribution, diversity, and function of these extremophiles in natural systems (Stetter *et al.*, 1990; Reysenbach & Shock, 2002). Microbial colonization of surfaces immediately adjacent to the spring source (0 m) was first detected 14 days after redirection (Fig. 5). The first colonizers at the source were *Stygiolobus*-like populations (Fig. 5), where three different *Stygiolobus*-like sequences (B21, B22, and B168) were detected at 0 and 2 m, each with 96–98% similarity to *Stygiolobus azoricus* (Fuchs *et al.*, 1996). This isolate is known to utilize H_2 as an electron donor and S° as an electron acceptor (Table 3). Dominant populations detected at 2 m on day 14 and at 0 m after day 14 included *Caldococcus*, *Caldisphaera*, and *Thermocladium*-like members of the *Crenarchaeota* (Fig. 5; Table 3). The nearest cultivated relatives of these populations are heterotrophic hyperthermophiles that require S° for optimal growth. This requirement for S° is consistently met at 0–2 m in *Succession Spring*.

Perhaps one of the major limitations of using energetic analyses to predict microbial distribution is the relative insensitivity of calculated ΔG_{rxn} values to changes in electron donor and acceptor concentrations (i.e. the reaction quotient, Q, in Equation #1). For example, the oxidation of H_2 with O_2 (Rxn 1, Table 2) is highly exergonic even under conditions with extremely low levels of O_2. The predicted energy yields at 10^{-24} M O_2(aq) are still – 64 kJ mol electron^{-1}. Thus, even at O_2 concentrations many orders of magnitude below the detection limit of most O_2 analytical methods, oxidation via O_2 would still be the most thermodynamically favored reaction. This is inconsistent with the fact that the 16S sequences detected near the source (0–2 m) were most closely related to obligate anaerobes that respire on S°. For example, members of the genus *Stygiolobus* are obligate anaerobes known to couple H_2 oxidation with the reduction of S° (Segerer *et al.*, 1991). The reduction of S° by H_2 under these conditions (Rxn 5, Table 2) would yield only –16 kJ mol electron^{-1}, which is significantly less favourable than most of the other reactions coupled with H_2 oxidation (Table 2). Furthermore, the characteristics of closest cultivated relatives to *Caldococcus, Caldisphaera*, and *Thermocladium*-like populations detected near the source suggest that these populations are anaerobic heterotrophs that also utilize S° as a terminal electron acceptor. Calculations indicate that the reduction of S° with a variety of C compounds results in significantly lower energy yields than reactions with other electron acceptors (data not shown; Amend & Shock, 2001). Consequently, factors other then energetic favorability result in the selection of S°-reducing populations under these conditions.

Formation of As(V)-hydrous ferric oxide microbial mats

The first visual and microscopic (SEM/EDAX) evidence of an As-rich hydrous ferric oxide (HFO) solid phase occurred by 14 d in the lower reaches of the outflow channel (10–14 m). During the next 89 days, the upper boundary of HFO deposition gradually progressed upstream, reaching 3 m by day 103 (Fig. 3). SEM/EDAX observations of the brown solid phase obtained during initial stages of formation (14 d at 12 m, Fig. 6A and B) showed clusters of cells with raspberry-like appearance similar to the coalescing spherules of amorphous As(V)-HFO observed in acid mine drainage by Morin *et al.* (2003). Thus, the origin of the As-rich HFO phase was apparently biogenic, its appearance correlating in time and space with microbial colonization. In addition, filtered (0.22 μM) source water incubated at spring temperatures confirmed that abiotic oxidation of Fe(II) did not occur over time scales necessary to control formation of these mats [<3 μM (method detection limit) over 30 min]. Furthermore, previous studies have shown that abiotic oxidation of Fe(II) at low pH was extremely slow (Nordstrom & Southam, 1997). The fact that no detectable losses of total dissolved Fe were observed during formation of HFO mat may be explained by the relatively slow deposition of HFO (on the order of weeks) compared to the large flux of Fe from the source (~500 μmol Fe min^{-1}) and the very short residence times of ~0.6 min over HFO mat positions.

Maturation of HFO microbial mats in *Succession Spring* was characterized by coverage of all surfaces with As-rich HFO (Figs 6C.D), including numerous ~1 μm diameter rod-shaped cells. EDAX of cells and surfaces encrusted with HFO showed mole ratios of As:Fe ranging from 0.60 to 0.74, similar to those observed in adjacent ASC springs (Langner *et al.*, 2001; Inskeep *et al.*, 2004) and very close to maximum values of 0.68 observed in synthetic solutions where 2-line ferrihydrite was precipitated in the presence of As(V) (Waychunas *et al.*, 1993). Total dissolution analysis yielded an average molar As:Fe ratio of 0.69, and essentially 100% of this phase was extractable with NH_4-oxalate (pH 3; Loeppert & Inskeep, 1996). The lability of this phase in oxalate was consistent with X-ray diffraction showing two broad Bragg peaks at d-spacings characteristic of 2-line ferrihydrite (0.15 and 0.27 nm). Furthermore, XANES and EXAFS analyses (Inskeep *et al.*, 2004) of several samples confirmed that (1) As(V) and Fe(III) were the predominant valence states of As and Fe in the solid phase; (2) arsenate was complexed to Fe(III) octahedral structures via primarily bidentate binding; and (3) the Fe(III) oxyhydroxide phase was poorly ordered, with significant disorder observed for the Fe-O-Fe coordination shell. While compositionally similar, HFO mats in three adjacent ASC springs, *Succession*, *Dragon*, and *Beowulf Springs*, exhibit considerable variability in micromorphology. Specifically, no filaments were observed in *Succession Spring* by day 103, while the HFO mats of *Dragon* and *Beowulf Springs* were comprised of an extensive network of filaments, often associated with flowing water (e.g. Eder & Huber, 2002). The relatively short duration of successional observations in the current study (103 d) may explain the predominance of rods vs. filaments.

The appearance of HFO phases at 10–14 m on day 14 (49 °C) correlated with the detection of bands B10 and BG39, whose sequences were closely related to *Thiomonas* sp. strain Ynys3 (98% similar to band B10; Dennison *et al.*, 2001; Table 3) and *Acidimicrobium* sp. strain Y0018 (98% similar to band BG39; Johnson *et al.*, 2003) (Fig. 5). The fact that close relatives of these populations have been shown to oxidize Fe(II), and that their detection in the spring coincided with HFO biomineralization, suggested that these populations were important in the initial formation of As(V)-rich HFO microbial mats. The detection of populations closely related to known Fe-oxidizers provides another line of evidence that HFO formation was not simply a result of passive Fe(II) oxidation and nucleation processes on cell walls. The biomineralization of HFO progressed upstream to 6 m on day 44 (Fig. 3), corresponding to the emergence of band B25, which is 98% similar to the sequence of *Metallosphaera prunae*. The *Metallosphaera* genus includes chemolithoautotrophs that are capable of growth on S° or Fe(II) (Fuchs

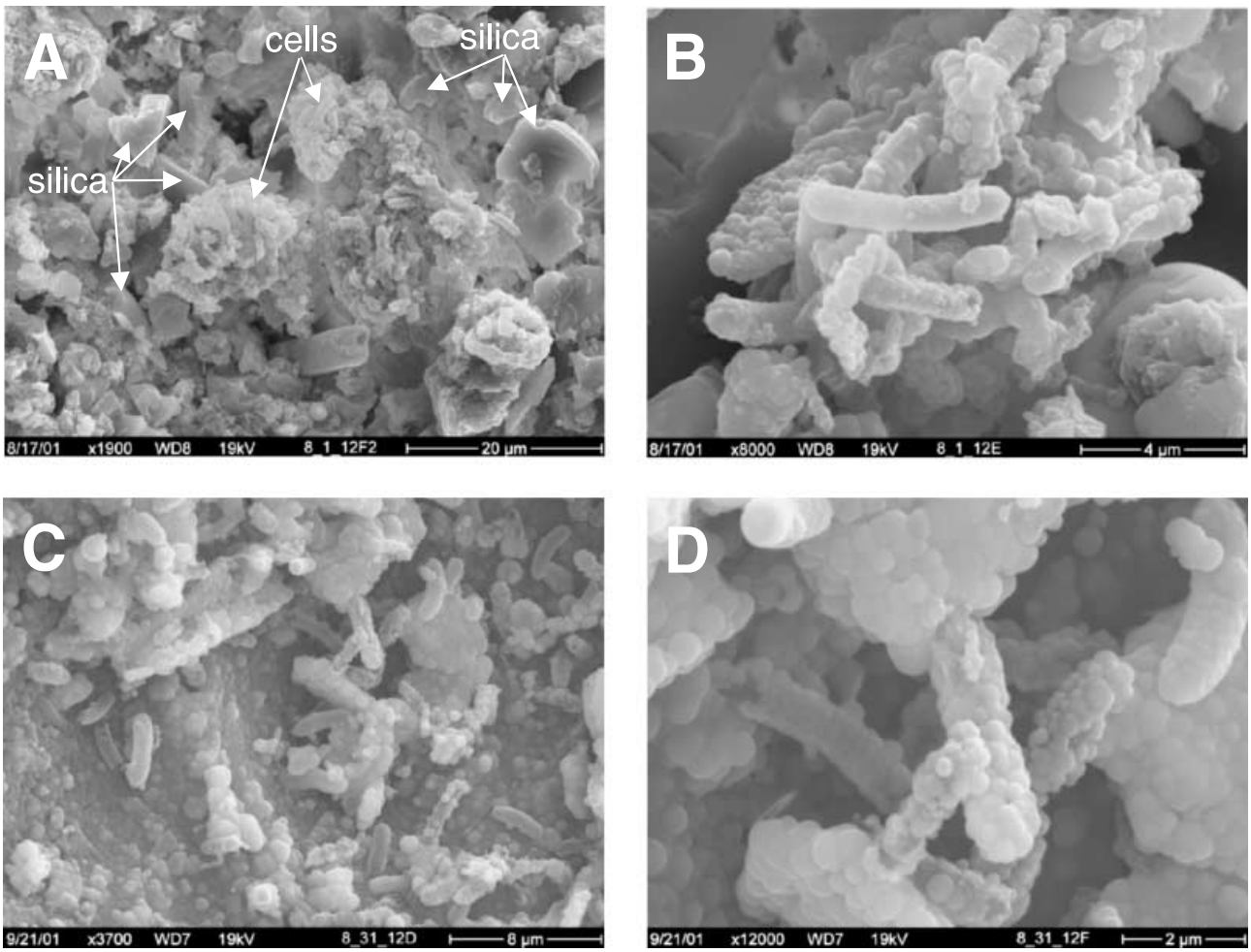

Fig. 6 Scanning electron micrographs (SEM) of As(V)-HFO phases deposited in the early stages (14 d) of microbial mat development at 12 m from spring discharge (panels A and B). Arrows in panel A point to clusters of cells that are coated with As(V)-HFO. Minerals immediately surrounding cell clusters are composed predominantly of silica. Panel B shows higher magnification image (8,000X) of cell clusters coated with As-rich HFO solid phase. The degree of HFO deposition at 12 m increased during the course of the study where by 44 d nearly all surfaces were coated with As-rich HFO (panels C and D).

et al., 1995; Peeples & Kelly, 1995). Thus, it appears that the *Metallosphaera*-like population was involved in HFO mat formation in a warmer region of the spring channel, as opposed to the *Thiomonas*-like population that was always detected at <56 °C. *Thiomonas* sp. are also aerobic, facultative chemolithotrophs capable of oxidizing reduced forms of S, As, and or Fe as possible electron donors (Moreira & Amils, 1997; Dennison *et al.*, 2001; Bruneel, 2004). Other sequences detected in the HFO mat include band B14, which was detected at 8 m on day 14 and was 99% similar to the sequence of an Fe(III)-reducing *Acetobacteraceae* strain Y008 obtained from Frying Pan Spring in Norris Basin (Johnson *et al.*, 2003). In addition, the sequence of band B179 detected in the HFO zone (12 m) on day 103 was 96% similar to the sequence of an aerobic bacteriochlorophyll producing *Acidisphaera rubrifaciens* (Hiraishi *et al.*, 2000) isolated from acidic hot springs in Japan.

The appearance of new microbial populations (e.g. *Thiomonas*-, *Acidimicrobium*-, *Metallosphaera*-like organisms) associated with HFO mat formation also correlated with further increases in As(III) oxidation rates observed at 7–13 m after 14 d (Fig. 2). The *Thiomonas*-like population detected in the HFO mat was closely related to two *Thiomonas* sp. strains (97% similarity to band B10; accession nos. AJ549219 and AJ549220; Bruneel *et al.*, 2003) shown to oxidize As(III) via an apparent detoxification mechanism. *Thiomonas* sp. have also been shown to possess aox genes, used in coding for an arsenite oxidase utilized for detoxification purposes (*Thiomonas* sp. VB-2002; accession no. AJ510263; Lebrun *et al.*, 2003; Muller *et al.*, 2003). Consequently, it is possible that the rapid rates of As(III) oxidation observed *in situ* may be partly due to similar mechanisms. In addition, Bruneel (2004) has recently isolated a *Thiomonas* strain that can use As(III) as the sole electron donor for energy generation. In summary, it is likely that both *Thiomonas* and *Hydrogenobaculum*-like populations contribute to As oxidation occurring down gradient. Energetic calculations also support the potential for chemolithotrophy

on As(III) in *Succession Spring* (Table 2). Thus, chemolithotrophic metabolism may be contributing to the oxidation of As(III) observed throughout the outflow channel and may be essential to formation of the As(V)-HFO microbial mat.

Detection of other novel microorganisms

Several archaeal and bacterial sequences (band numbers BG2, BG6, BG11, and BG12) detected in the spring after 5 days exhibited poor matches (<92%) to sequences from previously characterized isolates (Table 3). The nearest cultivated relatives corresponding to these sequences included *Thermofilum pendens* (89% similarity to BG2; Kjems *et al.*, 1990), *Aeropyrum pernix* strain OH1 (89% similarity to BG11; Nomura *et al.*, 2002), *Marinithermus hydrothermalis* (90% similar to BG6; Sako *et al.*, 2003), and a nonthermophilic planctomycete strain 567 (92% similar to BG12, Griepenburg *et al.*, 1999). The microorganisms represented by these sequences are likely members of novel genera and possibly novel families or orders of thermoacidophiles. Until these organisms are cultivated their physiologies can only be inferred from the environments in which they are detected. Recent efforts to clone 16S rDNA from ASC springs and soils in Norris Basin revealed many sequences similar to bands BG2, BG11, and BG12 (>98%, e.g. accession nos. AF325186, AF391991, AF391976), suggesting that related microorganisms represented by these sequences are widespread throughout Norris Geyser basin.

Microbial species distribution and community development

One of the primary goals of this work was to elucidate the geochemical and physical attributes important in controlling the distribution of microbial populations in geothermal systems. In turn, we are interested in how population distribution and community diversity are related to the functional processes that define different spatial or temporal habitats. Two previous studies in geochemically similar ASC springs show some agreement with the populations observed over 103 days in *Succession Spring*; however, distinct differences in populations are apparent among ASC springs (Jackson *et al.*, 2001; Inskeep *et al.*, 2004), indicating that even in these reasonably simple and similar communities, spatial and temporal heterogeneity yield different patterns of microbial community structure. In the current study, the function of specific microbial populations was inferred by simultaneously monitoring the development of microbial communities and coincident changes in geochemistry after spring redirection. This approach proved to be extremely useful for developing a reasonably thorough understanding of the geochemical processes associated with specific microbial populations detected as a function of time and space.

For example, the initial establishment of chemolithotrophic microorganisms dependent on H_2 near the spring source, followed by the development of a more complex community including heterotrophs, was supported by known physiologies of microorganisms closely related to those detected in the spring and by thermodynamic calculations based on spring geochemistry. Specifically, initial colonization by chemolithotrophic *Hydrogenobaculum* and *Stygiolobus*-like populations near the source was followed by appearance of populations related to heterotrophic *Caldococcus, Caldisphaera*, and *Thermocladium* organisms. These probable heterotrophs are likely dependent on C substrates provided by autotrophic organisms and a readily available source of elemental S. Given the relative simplicity of these communities, it may be possible to identify whether such relationships influence spatial and temporal population dynamics, and whether these interspecies relationships are an important selection force in the evolution of adapted populations.

Immediately down gradient of the S° depositional zone, a significant shift away from those populations that may utilize H_2S, S°, and H_2 as electron donors is expected. When concentrations of these constituents decline, As(III) and Fe(II) may then serve as important electron donors supporting nonphotosynthetic primary production. The energy yields for the oxidation of As(III) and Fe(II) via O_2 are significant at -61 kJ mol electron^{-1} and -32 kJ mol electron^{-1}, respectively (Rxns. 17 and 21, Table 2). The deposition of As(V)-rich HFO correlated with the appearance of *Thiomonas, Acidimicrobium*, and *Metallosphaera*-like populations whose closest cultivated relatives have been shown to oxidize Fe(II) and/or As(III) (Dennison *et al.*, 2001; Peeples & Kelly, 1995; Bruneel *et al.*, 2003; Johnson *et al.*, 2003). Several potentially important bacterial and archaeal sequences detected in the HFO mat following initial colonization were not closely related to 16S rDNA sequences from previously characterized organisms, and their physiologies are essentially unknown. Further work is necessary to understand the role of these populations in HFO mat development and the interspecies relationships that may contribute to defining community structure. The oxidation of Fe(II) and As(III) down gradient of spring environments that are dominated by more reduced species such as H_2, H_2S and S° demonstrates the importance of chemical energy gradients in establishing distinct community structure as a function of distance from spring discharge.

The acid-sulphate-chloride geothermal springs of Norris Basin, YNP, are the primary subject of a current Microbial Observatory project focused on the study of thermophilic chemolithotrophic microorganisms. Continuing work on ASC springs in Norris Basin will utilize the geochemical and phylogenetic information gained from this study to design enrichment environments for isolating and characterizing uncultured microorganisms detected in *Succession* and other ASC springs (Jackson *et al.*, 2001; Inskeep *et al.*, 2004). Additional effort will focus on defining functional linkages among individual microbial populations and the biogeochemical processes mediating Fe and As speciation and subsequent biomineralization of As-rich HFO phases.

ACKNOWLEDGEMENTS

The authors appreciate support for this research from the Thermal Biology Institute (NASA Project NAG5-8807) and the Montana Agricultural Experiment Station (Project 911398). The authors appreciate collaboration with Dr Tim McDermott on a currently funded National Science Foundation Microbial Observatory project (MCB-0132022) and further acknowledge partial summer salary support from this project for WPI during 2003.

REFERENCES

Allison JD, Brown DS, Novo-Gradac KJ (1991) MINTEQA2/PRODEFA2, A geochemical assessment model for environmental systems: version 3.0. User's manual. Environmental Research Laboratory, Office of Research and Development, USEPA, Athens, Georgia.

Altschul SF, Madden TL, Schäffer AA, Zhang J, Zhang Z, Miller W, Lipman DJ (1997) Gapped BLAST and PSI-BLAST: a new generation of protein database search programs. *Nucleic Acid Research* **25**, 3389–3402.

Amend JP, Shock EL (2001) Energetics of overall metabolic reactions of thermophilic and hyperthermophilic archaea and bacteria. *FEMS Microbiology Reviews* **25**, 175–243.

APHA (1998) 4500-S^{2-} D. Sulfide. In *Standard Methods for the Examination of Water and Wastewater* (eds Clesceri LS, Greenberg AE, Eaton AD). American Public Health Association, Washington, D.C, pp. 4–165–166.

Ball JW, McCleskey RB, Nordstrom DK, Holloway JM, Verplanck PL (2002) Water-chemistry data for selected springs, geysers, and streams in Yellowstone National Park, Wyoming 1999–2000. United States Geological Survey Open File Report 02-382, Boulder, CO.

Brock TD, Brock ML (1969) Recovery of a hot spring community from a catastrophe. *Journal of Phycology* **5**, 75–77.

Bruneel O (2004) Contribution to the study of the geochemical and bacteriological mechanisms in the transport of mining pollution at the site of Carnoulès (Gard, France). PhD Thesis, University Montpellier II, France.

Bruneel O, Personné JC, Casiot C, Leblanc M, Elbaz-Poulichet F, Mahler BJ, Le Flèche A, Grimont PAD (2003) Mediation of arsenic oxidation by *Thiomonas* sp. in acid-mine drainage (Carnoulès, France). *Journal of Applied Microbiology* **95**, 492–499.

Dennison F, Sen AM, Hallberg KB, Johnson DB (2001) Biological versus abiotic oxidation of iron in acid mine drainage waters: an important role for moderately acidophilic, iron-oxidising bacteria. In *Biohydrometallurgy: Fundamentals, Technology, and Sustainable Development, Part B* (eds Ciminelli VST, Garcia O Jr.,). Elsevier Science B.V., Amsterdam, Netherlands, pp. 493–501.

Donahoe-Christiansen J, D'Imperio S, Jackson CR, Inskeep WP, McDermott TR (2004) Arsenite-oxidizing *Hydrogenobaculum* strain isolated from an acid-sulfate-chloride geothermal spring in Yellowstone National Park. *Applied and Environmental Microbiology* **70**, 1865–1868.

Eary LE (1992) The solubility of amorphous As_2S_3 from 25 to 90 °C. *Geochimica et Cosmochimica Acta* **56**, 2267–2280.

Eder W, Huber R (2002) New isolates and physiological properties of the *Aquificales* and description of *Thermocrinis albus* sp. nov. *Extremophiles* **6**, 309–318.

Ferris MJ, Muyzer G, Ward DM (1996) Denaturing gradient gel electrophoresis profiles of 16S rRNA-defined populations inhabiting a hot spring microbial mat community. *Applied and Environmental Microbiology* **62**, 340–346.

Ferris MJ, Nold SC, Revsbech NP, Ward DM (1997) Population structure and physiological changes within a hot spring microbial mat community following disturbance. *Applied and Environmental Microbiology* **63**, 1367–1374.

Fuchs T, Huber H, Burggraf S, Stetter KO (1996) 16S rDNA-based phylogeny of the archaeal order sulfolobales and reclassification of *Desulfurolobus ambivalens* as *Acidianus ambivalens* comb. nov. *Systematic and Applied Microbiology* **19**, 56–60.

Fuchs T, Huber H, Teiner K, Burggraf S, Stetter KO (1995) *Metallosphaera prunae* sp. nov., a novel metal-mobilizing, thermoacidophilic *Archaeum*, isolates from a uranium mine in Germany. *Systematic and Applied Microbiology* **18**, 560–566.

Gihring TM, Druschel GK, McCleskey RB, Hamers RJ, Banfield JF (2001) Rapid arsenite oxidation by *Thermus aquaticus* and *Thermus thermophilus*: field and laboratory investigations. *Environmental Science and Technology* **35**, 3857–3862.

Griepenburg U, Ward-Rainey N, Mohamed S, Schlesner H, Marxsen H, Rainey FA, Stackebrandt E, Auling G (1999) Phylogenetic diversity, polyamine pattern and DNA base composition of members of the other *Planctomycetales*. *International Journal of Systematic Bacteriology* **49**, 689–696.

Helz GR, Tossell JA, Charnock JM, Pattrick RAD, Vaughan DJ, Garner CD (1995) Oligomerization in As (III) sulfide solutions: theoretical constraints and spectroscopic evidence. *Geochimica et Cosmochimica Acta* **59**, 4591–4604.

Hiraishi A, Matsuzawa Y, Kanbe T, Wakao N (2000) *Acidisphaera rubrifaciens* gen. nov., sp. nov., an aerobic bacteriochlorophyll-containing bacterium isolated from acidic environments. *International Journal of Systematic and Evolutionary Microbiology* **50**, 1539–1546.

Horikoshi K, Grant WD (1998) *Extremophiles, Microbial Life in Extreme Environments*. John Wiley & Sons Inc, New York.

Huber R, Huber H, Stetter KO (2000) Towards the ecology of hyperthermophiles: biotopes, new isolations strategies and novel metabolic properties. *FEMS Microbiology Reviews* **24**, 615–623.

Inskeep WP, Macur RE, Harrison G, Bostick BC, Fendorf S (2004) Biomineralization of As (V)-hydrous ferric oxyhydroxide in microbial mats of an acid-sulfate-chloride geothermal spring, Yellowstone National Park. *Geochimica et Cosmochimica Acta* **68**, 3141–3155.

Jackson CR, Langner HW, Donahoe-Christiansen J, Inskeep WP, McDermott TR (2001) Molecular analysis of microbial community structure in an arsenite-oxidizing acidic thermal spring. *Environmental Microbiology* **3**, 532–542.

Johnson DB, Okibe N, Roberto FF (2003) Novel thermo-acidophilic bacteria isolated from geothermal sites in Yellowstone National Park: physiological and phylogenetic characteristics. *Archives of Microbiology* **180**, 60–68.

Kjems J, Leffers H, Olesen T, Ingelore H, Garrett RA (1990) Sequence, organization and transcription of the ribosomal RNA operon and the downstream tRNA and protein genes in the archaebacterium *Thermofilum pendens*. *Systematic and Applied Microbiology* **13**, 117–127.

Kostov I, Kostov RI (1999) *Crystal Habits of Minerals*. Prof. Marin Drinov Academic Publishing House & Pensoft Publishers, Sofia, Bulgaria.

Langner HW, Jackson CR, McDermott TR, Inskeep WP (2001) Rapid oxidation of arsenite in a hot spring ecosystem, Yellowstone National Park. *Environmental Science and Technology* **35**, 3302–3309.

Lebrun E, Brugna M, Baymann F, Muller D, Lièvremont D, Lett MC, Nitschke W (2003) Arsenite oxidase, an ancient bioenergetic enzyme. *Molecular Biology and Evolution* **20**, 686–693.

Loeppert RH, Inskeep WP (1996) Iron. In *Methods of Soil Analysis. Part 3. Chemical Methods* (ed. Sparks DL). Soil Science Society of America, Madison, WI, pp. 639–664.

Madigan MT, Martinko JM, Parker J (2002) *Brock Biology of Microorganisms*. Prentice Hall, NJ.

Moreira D, Amils R (1997) Phylogeny of *Thiobacillus cuprinus* and other mixotrophic Thiobacilli: proposal for *Thiomonas* gen. nov. *International Journal of Systematic Bacteriology* **47**, 522–528.

Morin G, Juillot F, Casiot C, Bruneel O, Personné JC, Elbaz-Poulichet F, Leblanc M, Ildefonse P, Calas G (2003) Bacterial formation of tooeleite and mixed arsenic (III) or arsenic (V) – iron (III) gels in the Carnoulès acid mine drainage in France: a XANES, XRD, and SEM study. *Environmental Science and Technology* **37**, 1705–1712.

Mukhopadhyay R, Rosen BP, Phung LT, Silver S (2002) Microbial arsenic: from geocycles to genes and enzymes. *FEMS Microbiology Reviews* **26**, 311–325.

Muller D, Lièvremont D, Simeonova DD, Hubert JC, Lett MC (2003) Arsenite oxidase *aox* genes from a metal-resistant β-proteobacterium. *Journal of Bacteriology* **185**, 135–141.

Nomura N, Morinaga Y, Kogishi T, Kim EJ, Sako Y, Uchida A (2002) Heterogeneous yet similar introns reside in identical positions of the rRNA genes in natural isolates of the archaeon *Aeropyrum pernix*. *Gene* **295**, 43–50.

Nordstrom DK, Archer DG (2003) Arsenic thermodynamic data and environmental geochemistry. In *Arsenic in Ground Water: Geochemistry and Occurrence* (eds Welch AH, Stollenwerk KG). Kluwer Academic publishers, Boston, pp. 1–25.

Nordstrom DK, Southam G (1997) Geomicrobiology of sulfide mineral oxidation. *Reviews in Mineralogy*. **35**, 361–390.

Peeples TL, Kelly RM (1995) Bioenergetic response of the extreme thermoacidophile *Metallosphaera sedula* to thermal and nutritional stresses. *Applied and Environmental Microbiology* **61**, 2314–2321.

Reysenbach AL, Shock E (2002) Merging genomes with geochemistry in hydrothermal ecosystems. *Science* **296**, 1077–1082.

Rosen BP (2002) Transport and detoxification systems for transition metals, heavy metals and metalloids in eukaryotic and prokaryotic microbes. *Comparative Biochemistry and Physiology* **133**, 689–693.

Sako Y, Nakagawa S, Takai K, Horikoshi K (2003) *Marinithermus hydrothermalis* gen. nov., sp. nov., a strictly aerobic, thermophilic bacterium from a deep-sea hydrothemal vent chimney. *International Journal of Systematic and Evolutionary Microbiology* **53**, 59–65.

Segerer AH, Trincone A, Gahrtz M, Stetter KO (1991) *Stygiolobus azoricus* gen. nov., sp. nov., represents a novel genus of anaerobic, extremely thermoacidophilic archaebacteria of the order *Sulfolobales*. *International Journal of Systematic Bacteriology* **41**, 495–501.

Shima S, Suzuki KI (1993) *Hydrogenobacter acidophilus* sp. nov., a thermoacidophilic, aerobic, hydrogen-oxidizing bacterium requiring elemental sulfur for growth. *International Journal of Systematic Bacteriology* **43**, 703–708.

Silver S (1996) Bacterial resistances to toxic metal ions-a review. *Gene* **176**, 9–19.

Spear JR, Pace NR (2004) Diversity of life at the geothermal subsurface–surface interface: the Yellowstone example. In *The Subseafloor Biosphere: American Geophysical Union Monograph* (ed. Wilcock W). AGU Geophysical Monograph Series. American Geophysical Union, Washington DC, pp. 339–350.

Stauffer RE, Jenne EA, Ball JW (1980) Chemical studies of selected trace elements in hot-spring drainages of Yellowstone National Park: US. *Geological Survey Professional Paper 1044-F. United States*. Government Printing Office, Washington D.C.

Stetter KO, Fiala G, Huber G, Huber R, Segerer A (1990) Hyperthermophilic microorganisms. *FEMS Microbiology Reviews* **75**, 117–124.

To TB, Nordstrom DK, Cunningham KM, Ball JW, McCleskey RB (1999) New method for the direct determination of dissolved Fe (III) concentration in acid mine waters. *Environmental Science and Technology* **33**, 807–813.

Waychunas GA, Rea BA, Fuller CC, Davis JA (1993) Surface chemistry of ferrihydrite: Part 1. EXAFS studies of the geometry of coprecipitated and adsorbed arsenate. *Geochimica et Cosmochimica Acta* **57**, 2251–2269.

Webster JG (1990) The solubility of As_2S_3 and speciation of As in dilute and sulphide-bearing fluids at 25 and 90 °C. *Geochimica et Cosmochimica Acta* **54**, 1009–1017.

Wilkie JA, Hering JG (1998) Rapid oxidation of geothermal arsenic (III) in streamwaters of the eastern Sierra Nevada. *Environmental Science and Technology* **32**, 657–662.

Xu Y, Schoonen MAA, Nordstrom DK, Cunningham KM, Ball JW (1998) Sulfur geochemistry of hydrothermal waters in Yellowstone National Park. I. The origin of thiosulfate in hot spring waters. *Geochimica et Cosmochimica Acta* **62**, 3729–3743.